Cassini CAPS identification of pickup ion compositions at Rhea

R. T. Desai[1,2,3], S. A. Taylor[1,2], L. H. Regoli[4], A. J. Coates[1,2], T. A. Nordheim[5], M. A. Cordiner[6], B. D. Teolis[7], M. F. Thomsen[8], R. E. Johnson[9], G. H. Jones[1,2], M. M. Cowee[10], J. H. Waite[7]

Corresponding author: R. T. Desai, Blackett Laboratory, Imperial College London, London, UK. (ravindra.desai@imperial.ac.uk)

[1]Mullard Space Science Laboratory,

Saturn's largest icy moon, Rhea, hosts a tenuous surface-sputtered exosphere composed primarily of molecular oxygen and carbon dioxide. In this Letter, we examine Cassini Plasma Spectrometer velocity space distributions near Rhea and confirm that Cassini detected nongyrotropic fluxes of outflowing CO_2^+ during both the R1 and R1.5 encounters. Accounting for this nongyrotropy, we show that these possess comparable alongtrack densities of $\sim 2\times10^{-3}$ cm^{-3}. Negatively charged pickup ions, also detected during R1, are surprisingly shown as consistent with mass 26±3 u which we suggest are carbon-based compounds, such as CN^-, C_2H^-, C_2^-, or HCO^-, sputtered from carbonaceous material on the moons surface. The negative ions are calculated to possess alongtrack densities of $\sim 5\times10^{-4}$ cm^{-3} and are suggested to derive from exogenic compounds, a finding consistent with the existence of Rhea's dynamic CO_2 exosphere and surprisingly low O_2 sputtering yields. These pickup ions provide important context for understanding the exospheric and surface-ice composition of Rhea and of other icy moons which exhibit similar characteristics

University College London, UK.

1. Introduction

Rhea is Saturn's largest icy moon with a radius of ∼764 km, and orbits within the sub-Alfvénic environment of Saturn's middle magnetosphere. As such, Rhea presents an archetype of the dominant satellite class at the outer planets, whose physical properties can be used to understand the formation and evolution of the giant planetary systems and, especially, their many moons.

A sputter-induced exosphere was first discovered to exist at Rhea by the Cassini spacecraft [Teolis et al., 2010], a phenomenon also present at Dione, Europa, Callisto, and Ganymede [Tokar et al., 2012; Hall et al., 1998; Carlson, 1999]. Rhea's and Dione's exospheres were also surprisingly found to host large quantities of CO_2 [Teolis & Waite, 2016], a characteristic shared with Callisto. Rhea's surface is predominantly water ice whilst also containing lesser quantities of darker non-ice constituents and trace compounds such as CO_2 [Clark et al., 2008]. Beneath this, Rheas gravitational field indicates a body existing away from hydrostatic equilibrium which might be differentiated [Tortora et al., 2016], and possibly hosts a subsurface water ocean [Hussmann et al., 2006].

Rhea is an unmagnetised body and acts to absorb incident magnetodisk plasma [Khurana et al., 2008; Roussos et al., 2008]. Ionised material can be directly picked up by the motional electric field and form "pickup ion" current systems which, with the resulting j×B force and density gradients associated with the plasma wake [Simon et al., 2012; Khurana et al., 2017], slows down the incident magnetoplasma causing field-line drap-

[2]Centre for Planetary Science at

ing and Alfvén wings. Pickup ions, as well as providing information on bulk and trace

UCL/Birkbeck, London, UK.

[3]Blackett Laboratory, Imperial College London, UK.

[4]Michigan University, Department of Space Science and Engineering, Michigan, USA.

[5]NASA-JPL/Caltech, Pasadena, California, USA.

[6]NASA Goddard Space Flight Center, Maryland, USA.

[7]Space Science and Engineering Division, Southwest Research Institute, Texas, USA.

[8]Planetary Science Institute, Tucson, Arizona, USA.

[9]Engineering Physics, University of Virginia, Charlottesville, USA.

[10]Los Alamos National Laboratory, Los Alamos, New Mexico, USA.

atmospheric constituents, impact the moon's plasma interaction and mass load Saturn's middle magnetosphere.

In a plasma flow, pickup ions will be accelerated to a maximum velocity of twice that of the bulk plasma and, in the plasma frame, will possess energies of

$$E_i = \frac{1}{2} m_i v_b^2 sin^2\theta, \quad (1)$$

where m_i is the pickup ion mass, v_b is the bulk plasma velocity in the initial rest frame, and θ is the angle between the bulk plasma velocity and the magnetic field [Coates et al., 1989].

At Rhea's orbit of $\sim$8.9 R_S, the Saturnian magnetic field is nominally dipolar and newly born ions will be accelerated perpendicularly to the magnetic field to execute rings in velocity space. If the size of the ion gyroradii significantly exceeds that of the pickup ion source region, the resultant distributions won't fill the entire ring and can be considered nongyrotropic.

Pickup ion distributions are inherently unstable and provide a source of free energy for plasma wave generation [Wu & Davidson, 1972]. These waves act scatter the distributions in pitch angle and energy, and heat ambient gyroresonant populations. Alfvén-cyclotron waves, generated by pickup ions, have been observed throughout Saturn's extended neutral cloud out to $\sim$8 Rs where the increased plasma beta (ratio of magnetic to thermal pressure) results in the Mirror Mode dominating [Russell et al., 2006; Meeks et al., 2016]. The magnetic signatures of mass loading have, however, not been reported in the vicinity of Rhea, despite increased O_2^+ abundances being observed at these radial distances [Martens et al., 2008].

In this *Letter*, we examine Cassini Plasma Spectrometer (CAPS) observations of pickup ions outflowing from Rhea with emphasis on further constraining the composition and origin of the negatively charged pickup ions detected by the CAPS Electron Spectrometer (ELS).

2. Velocity Space Analysis

The CAPS Ion Mass Spectrometer (IMS) and CAPS Electron Spectrometer (ELS) [Young et al., 2004] were designed to measure low energy ions and electrons in the ranges of 1 eV to 50.3 keV and 0.6 eV to 28.8 keV, respectively. CAPS is located on an actuator which was held fixed during the Rhea flybys. Figure 1 shows the CAPS observations during the targeted R1 enounter on 26 November 2005 and the non-targeted R1.5 encounter on 30 August. Closest approach occurred at 765 km and 5736 km, respectively, and both flybys occurred behind the moon, thus providing the opportunity to observe outflowing material.

During both encounters, a marked drop-out in ion and electron fluxes occurs as Cassini traversed the moon's plasma wake. During R1, distinct plasma populations are visible in the IMS spectrogram around 22:33 UT at $\sim$2.5 keV, and during R1.5 a similar population is observed at 01:32 UT at $\sim$3.5 keV. In the ELS spectrogram, a distinct plasma population is visible at 22:41 UT at $\sim$1.6 keV, and a differenced plot, obtained by averaging the counts on anodes oriented away from 90° pitch angle (anodes 2, 3, 6, 7), and subtracting these from anode 3, reveals this signature as analogous to the IMS signatures. These respective plasma populations have been identified as positively and negatively charged pickup ions

deriving from Rhea and provided evidence for the moon's tenuous exosphere [Teolis et al., 2010].

The IMS and ELS utilise electrostatic analysers to energy select charged particles, and the characteristic velocity imparted to newly created ions by the pickup process allows CAPS to discriminate between pickup ions of different masses. Figure 2 shows an IMS and ELS energy sweep corresponding to when these pickup ions were detected. The data are transformed into velocity space using the mass of anticipated pickup ions and projected onto planes which are parallel and perpendicular to the magnetic field and $-v \times B$ electric field, as measured by Cassini [e.g. Wilson et al., 2010]. The spacecraft and plasma velocity are subtracted, leaving the measurements in the pickup ion rest frame and a contour representing the anticipated pickup ion ring distribution is overlaid, as predicted by Equation 1.

During R1 and R1.5, the pickup ions observed by the IMS appear consistent with masses 40±4 u and 46±4 u, respectively. This uncertainty derives from the width of the IMS energy bins and the plasma velocity which varies between ∼55 and ∼60 km/s during R1, and ∼55 and ∼65 km/s during R1.5, see Wilson et al. [2010]. The pickup ions arrive with near-zero velocity parallel to the B-field as anticipated for pickup within a dipolar pickup geometry and are therefore attributed to CO_2^+, a conclusion previously reached by Teolis & Waite [2016].

The pickup ions possess varying velocities parallel to the electric field indicating they are highly nongyrotropic and exist within slightly different locations in phase space. During both encounters the pickup ions appear shifted compared to the predicted velocity con-

tours, the most likely explanation being that the plasma conditions were different closer to the moon, where and when the ions were produced, compared to at the time and location of their detection. In Figure 3, the nominal trajectories of outflowing positive and negative pickup ions are shown, calculated using Cassini field and plasma measurements. The CO_2^+ trajectories can be seen to correspond to where the respective detections were made during both R1 and R1.5.

The nongyrotropic nature of these distributions also becomes evident when examining these trajectories as they demonstrate how the pickup ions are only able to occupy a finite amount of the 2π velocity-ring space at any given instance. This also explains why the pickup ions are only observed over a finite time period as the pickup ion phase angle changes closer to the moon to where the CAPS finite FOV did not cover. Spatial variations in the ion production rate, due to the spatial distribution of the exospheric neutral density, could also contribute to this effect.

The identification of CO_2^+ on both the Rhea encounters raises interesting questions regarding the lack of O_2^+ pickup ions, as observed at Dione by Cassini [Tokar et al., 2012]. The IMS spectra shown in Figure 4 do, however, feature a shoulder on the main corotational plasma distribution near $\sim$2 keV which, when closer to Rhea (not shown), appears similar to the O_2^+ pickup ion detections reported by Tokar et al. [2012]. It is, however, difficult to differentiate this from the corotational plasma at Rhea's orbit, which exhibits a greater spread in energy compared to at Dione. Rhea's CO_2 and O_2 exosphere has been measured insitu by Cassini's Ion and Neutral Mass Spectrometer [Teolis & Waite, 2016], and the O_2 production rates have notably been determined to be significantly ($\sim$300

times) lower than that predicted from the sputtering of pure water-ice, and are consistent with the presence of significant surface impurities.

The consistency of these identifications with the analysis and exospheric modelling results reported by Teolis & Waite [2016], validates the use of the pickup ions velocity as a means of identifying composition, a method which will now be applied to analyse the negatively charged pickup ions.

The CAPS-ELS is capable of detecting negatively charged ions [Coates et al., 2007], and Teolis et al. [2010] reported that the negatively charged pickup ions detected during R1 were likely comprised of O^-. While initially reported as produced from electron attachment to atmospheric species, the inefficiency of this process was highlighted in a subsequent study [Teolis & Waite, 2016; Itikawa, 2009], and it was consequently suggested that these were likely produced by surface mediated process such as sputtering. In Figure 1 and 2, these detections appear above the anticipated O^- energy by $\sim$15 km/s which corresponds to an energy discrepancy of $\sim$500 eV. These detections therefore appear consistent with a heavier species of mass 26$\pm$3 u. It is, however, possible for pickup ions to be accelerated to increased energies by a number of processes, which are now examined:

- Intense plasma waves have been observed at Rhea [Santolík et al., 2011], and right-hand polarised Alfvén-cyclotron waves, which would gyroresonantly interact with O^-, could be produced by negatively charged pickup ions [Desai et al., 2017b]. These however feed of the free energy from the pickup ions and this effect could not be significant over such a short time period.

• Specular reflection from the lunar surface has been observed to accelerate solar wind ions to three times that of the bulk plasma velocity [Saito et al., 2008]. This is however judged unlikely at Rhea due to high water-group photo-detachment rates in Saturn's magnetosphere [Coates et al., 2010] precluding negatively charged O^- existing in abundance as an ambient magnetospheric population.

• Sputtering can result in energy being transferred to the sputter products. O^- sputtering experiments have, however, shown this to be too inefficient to account for the velocity discrepancy discovered herein [Tang et al., 1996].

• Previous theoretical studies have predicted large negative surface potentials at Rhea up to several hundred volts [Roussos et al., 2010; Nordheim et al., 2014] and observations during the Rhea R2 flyby appear to support this [Santolík et al., 2011]. However, for surface potentials to explain the observed energy discrepancy, a negative surface potential of 500V would have to occur uniformly over a large region of Rhea's surface. Given that the theoretical studies have predicted surface potentials which vary strongly depending on surface location, this is not considered likely.

• The bulk plasma velocity is predicted to vary in the vicinity of Rhea and in particular on the Saturn-facing hemisphere [Roussos et al., 2008]. The CAPS plasma velocity measurements during R1 were, however, obtained in this region and do not show this effect to be significant [Wilson et al., 2010].

The apparent inconsistency with O^- pickup ions raises two possibilities. Firstly, the signature could be produced by an electron beam oriented perpendicularly to the magnetic field. The longevity of this signatures above the background populations, its spatial

occurrence, and the similarity to the unambiguous positive pickup ion signatures, are however highly indicative of negatively charged pickup ions of mass 26±3 u, of a type not previously considered.

3. Origin of the Negative Ions

Heavier negative pickup ions could result from carbon-based compounds with positive electron affinities (EA), such as CN^-, C_2H^-, C_2^-, or HCO^-, being produced via sputtering of the moon's surface. Spectroscopic observations of Rhea at $\leq$5.2 μm wavelengths have revealed unusually dark material which is consistent with the presence of either tholin (C-, H-, N-, O- bearing) and/or iron (Fe- bearing) compounds [Ciarniello et al., 2011; Stephan et al., 2012; Scipioni et al., 2014]. This material is also present at Dione, Phoebe, Iapetus, Hyperion, Epimetheus and throughout Saturn's F-ring, thus implying a common process occurring throughout these icy satellites [Clark et al., 2008]. Dark tholin-like material is also apparent in spectroscopic observations of the Galilean icy moons, which is thought to be comprised of hydrocarbon or cyanide compounds [McCord et al., 1998]. An abundance of electrons are also anticipated near Rhea's negatively charged surface which could readily attach onto electrophillic molecules.

Visual Infrared Mapping Spectrometer (VIMS) observations of Rhea have shown that an ~1% tholin-type admixture could explain unidentified features in the near-infrared [Ciarniello et al., 2011]. It therefore initially appears surprising that such a trace constituent would be observed outflowing in significant quantities. The pickup ion trajectories, however, shown in Figure 3, demonstrate how pickup ions originating from different regions in Rhea's exosphere become concentrated in phase space when observed, a phenomenon

which appears enhanced for heavier species due to their larger gyroradii. This could explain why a trace heavier species might preferentially be detected.

VIMS observations of Rhea's surface are also derived from the top few microns and exogenous material might not have penetrated this far. A thin carbonaceous surface coating on the moon, possibly only a few monolayers thick, could therefore consist of significantly larger fraction of this unidentified dark material than is apparent from remote observations. This could have been deposited from magnetospheric plasma and dust populations, or been delivered by micrometeorite, cometary and interplanetary particles raining into the Saturn system [Clark et al., 2008; Stephan et al., 2012]. At Rhea, the spatial distributions of the unidentified material indeed suggest an external origin, with higher concentrations on the leading and trailing hemispheres pointing to magnetospheric dust and plasma deposition, respectively [Clark et al., 2008; Scipioni et al., 2014].

Dark spots are also observed near Rhea's equator which are associated with surface disruptions [Schenk et al., 2011]. The negative pickup ions map back to near Rhea's equatorial regions and the possibility that endogenic carbon-rich material could have been released onto the surface via impact events such as the cause of the Inktomi impact crater, or the discolored spots, or from further large-scale geologocial resurfacing [e.g. Stephan et al., 2010], cannot be discounted.

It is possible for tholin-type compounds to be incorporated into the ice from when the moon formed. Compounds such as C_2H_2, CH_3OH and HCN appear ubiquitously within cometary ices at $\sim$1% of H_2O abundances, thus signifying their presence in the protosolar accretion disk from which the giant planetary systems formed [Mumma & Charnley, 2011].

Teolis & Waite [2016] go on to predict the quantity of carbon atoms in Rhea's surface ice to be as high as 13% that of H_2O and processes such as photolysis, radiolysis, and heating could act to process the chemical state of such compounds, whether endogenic or exogenic to Rhea.

The CN^- (EA = 3.8 eV), C_2H^- (EA = 3.0 eV) and C_2^- (EA = 3.3 eV) anions can be produced from electrons impacting compounds such as hydrogen cyanide, acetylene and diacetylene [Inoue, 1966; May et al., 2008]. Graphite-compounds could be created through radiation bombardment and surface chemistry [Lifshitz et al., 1990; McCord et al., 1998], which could produce C_2^-. Sputtering experiments indeed predict the efficient production of the $C_2H_x^-$ anions from hydrocarbon compounds [Johnson et al., 1992], and these are suggested as candidate sputter products at Europa [Johnson et al., 1998]. Carbon chain anions have also possibly been observed at Comet Halley [Cordiner & Charnley, 2014] and exist elsewhere in Saturn's magnetosphere, amongst carbon-rich compounds in Titan's ionosphere [Desai et al., 2017a]. The HCO^- (EA = 0.31 eV) anion could possibly be formed by deprotonation or dissociative electron attachment of H_2CO or CH_3OH. Further study of the sputtering of carbon-rich ejecta from ices representative of the icy moons of Saturn and Jupiter, could surely provide further insight into which sputtering rates are significant with regards to these anions.

Although the aforementioned negative pickup ions appear inconsistent with O^-, it should be noted that in the differenced ELS spectrogram displayed in Figure 1, further signatures also consistent with negative pickup ions are present earlier in time at a lower energy. Although too brief to conclusively identify these as negative ions, this

might represent the same pickup ion population dispersed in energy via interactions with a surface-generated electric field as observed at the Earth's moon [Poppe et al., 2012], or indeed could correspond to O^- pickup ions given their location in phase space, see Figure 3.

4. Densities & Escape Rates

Figure 4 shows IMS energy spectra during R1 and R1.5 and the ELS spectrum during R1, corresponding to the pickup ion detections. The ion background is fitted using a Maxwellian water-group velocity distribution which appears to better match the data during R1.5 when Cassini was farther from Rhea's plasma interaction. In either instance the pickup ion detections are clearly identifiable and these fits are sufficient to isolate the pickup ion populations. A lower energy hydrogen population is also present, as well as further high energy populations evident at >4 keV. These are not considered for this analysis.

The ELS spectrum shows two distinct electron populations at low and high energies which are represented using a double Kappa distribution [Schippers et al., 2009]. A significant amount of intermediary electrons are also present which are also approximated by a broad Kappa distribution. The proximity to Rhea's plasma interaction, as well as multiple possible photoelectron populations [Taylor et al., 2017], result in significant variabilities in the electron spectrum during R1. The negatively charged pickup ion population consistently remains above the background throughout this variability, see Figure 1.

The nongyrotropic pickup ion densities are calculated using an expression derived for partially-filled ring-velocity distributions. In the plasma frame, the pickup ions can be expressed relative to the magnetic field as

$$f(v) = \frac{n}{\Delta\phi v_{b\perp}} \delta(v_{perp} - v_{b\perp}) \delta(v_{\parallel} - v_{b\parallel}), \quad (2)$$

where $\Delta\phi = 2\pi$ in the case of a gyrotropic ring [Wu & Davidson, 1972].

Pickup ion trajectories derived from the extrema of Rhea's exosphere, see Figure 3, are used to estimate that the pickup ions are able to fill $\sim \pi/4$ of velocity space, see Figure 3. This can be expressed in the spacecraft frame as

$$f(v) = \frac{n}{\Delta\phi v_{b\perp}} \delta(v_b - v_c) \delta v_{b\parallel}, \quad (3)$$

where v_c is the velocity corresponding to the CAPS energy bin in which the pickup ions were detected. The spacecraft velocity is removed for an inertial reference frame. The pickup ion density, n, can then be calculated from the count rate, R_c by the expression,

$$n = \frac{R_c \Delta\phi}{v_b \varepsilon A \Delta\phi_c}, \quad (4)$$

where the area of acceptance $A = 0.33 cm^{-2}$, the CAPS phase angle coverage $\Delta\phi_c = \pi/2$, and ε is the Microchannel Plate (MCP) efficiency. An MCP efficiency of 0.46 is used for the CO_2^+ pickup ions and 0.50 for the negatively charged pickup ions [Tokar et al., 2012; Stephen & Peko., 2000].

Figure 4 shows the resulting IMS and ELS along-track densities. The CO_2^+ densities peak at $\sim 2.5 \times 10^{-3}$ cm^{-3} whereas the negatively charged pickup ions peak at values nearly an order of magnitude lower at $\sim$5x10^{-4}. The CO_2^+ densities during R1 are also calculated

assuming a gyrotropic distribution to demonstrate how such an assumption significantly overestimates abundances.

Whilst Rhea's exosphere has shown to be dynamic and variable, the CO_2^+ densities can be integrated over the hemisphere of the moon where the motional electric field will result in ion escape, to calculate approximate global escape rates. Assuming uniform ionisation, this results in an estimated $\sim 4.6\times10^{20}$ CO_2^+ s^{-1} escaping the moon during R1 and $\sim 5.7\times10^{20}$ CO_2^+ s^{-1} during R1.5. This rate is compatible with the varying CO_2 production rates resulting from the model of Teolis & Waite [2016]. This is also $\sim$0.25 times that predicted at Dione which experiences more intense plasma bombardment due to being located deeper inside Saturn's magnetosphere [Wilson et al., 2017]. A similar calculation can be performed for the negative ions which results in an outflow rate of $\sim 5.4\times10^{19}$ s^{-1}.

It should be noted that these rates are only an estimate as studies have shown highly varying dynamical processes at Rhea's magnetospheric interaction at small or intermediate scales, and such dynamics may "destroy" or disperse the smooth paths of pick-up ions with small or moderate-sized gyroradii [Roussos et al., 2012]. It is therefore not clear precisely which density should be used to represent globally averaged ion production rates.

The outflowing pickup ions will contribute to magnetospheric ion populations. Rhea's CO_2 exosphere may therefore provide a source of the 44 u ions, or the carbon and oxygen ions via dissociative reactions, identified at radial distances of $<$20 R_S [Christon et al., 2015]. If the breakup is sufficiently fast, this may provide some explanation for the elevated O_2^+ levels reported by Martens et al. [2008] at Rhea's orbit.

Further analysis of the generation of instabilities associated with nongyrotropic pickup ions, in a plasma beta regime representative of Rhea's plasma environment, is required to understand whether the magnetic signature of this mass loading might be visible.

5. Summary & Conclusions

This study has analysed the composition, density and outflow rates of positively and negatively charged pickup ion distributions at Saturn's icy moon Rhea and determined the following:

- CAPS-IMS observed nongyrotropic fluxes of CO_2^+ pickup ions during the R1 and R1.5 encounters with comparable alongtrack densities of $\lesssim 2\times10^{-3}$cm^{-3}.
- The R1 CAPS-ELS detections, previously identified as deriving from the pickup of O^-, are shown as consistent with a heavier species of mass 26±3u. These are consequently identified as negatively charged carbon-based compounds produced from tholin-type material on Rhea's surface.
- The negatively charged pickup ions are suggested to consist of CN^-, C_2H^-, C_2^- or HCO^-, resulting from the dark material observed at Rhea and throughout the icy moons of Saturn.
- The negatively charged ions were observed with alongtrack densities of $\lesssim 5\times10^{-4}$ cm^{-3}.
- Possible further negative ion signatures are also identified which could represent dispersion in energy as a result of surface charging or a further population of O^- pickup ions.

This study provides context for understanding the exospheric and surface compositions and plasma interaction of Rhea as well as other icy satellites in the outer solar system. The trace constituents in Rhea's surface ice, and also at other Saturnian and Jovian icy moons, are largely unconstrained and it remains to be determined just how similar or different these ices are to each other or indeed to ices formed elsewhere in the solar system such as those within comets and further icy bodies.

Acknowledgments. RTD acknowledges STFC Studentship No.1429777. AJC and GHJ acknowledge support from the STFC consolidated grants to UCL-MSSL ST/K000977/1 and ST/N000722/1. The Cassini CAPS data used are available on the Planetary Database System (PDS) or upon reasonable request.

References

Carlson, R. W. 1999, A Tenuous Carbon Dioxide Atmosphere on Jupiter's Moon Callisto, *Science*, 283, 820

Christon, S. P., Hamilton, D. C., Plane, J. M. C., et al. 2015, Journal of Geophysical Research (Space Physics), 120, 2720

Ciarniello, M., Capaccioni, F., Filacchione, G., et al. 2011, Hapke modeling of Rhea surface properties through Cassini-VIMS spectra, *Icarus*, 214, 541

Clark, R. N., Curchin, J. M., Jaumann, R., et al. 2008, Compositional mapping of Saturns satellite Dione with Cassini VIMS and implications of dark material in the Saturn system, *Icarus*, 193, 372

Coates, A. J., Crary, F. J., Lewis, G. R., et al. 2007, Discovery of heavy negative ions in Titans ionosphere, *GRL*, 34, L22103

Coates, A. J., Johnstone, 1989, A. D., Wilken, B., Jockers, K., & Glassmeier, K.-H. 1989, Velocity space diffusion of pickup water group ions at Comet-Halley, *JGR*, 94, 9983

Coates, A. J., Jones, G. H., Lewis, G. R., et al. 2010, Negative Ions in the Enceladus Plume, *Icarus*, 206, 618

Cordiner, M. A., & Charnley, S. B. 2014, Negative ion chemistry in the coma of comet 1P-Halley, *MPS*, 49, 21

Desai, R. T., Cowee, M. M., Wei, H., et al., 2017, Hybrid simulations of positive and negatively charged pickup ions and cyclotron wave generation at Europa, *JGR*, 122, 10.

Desai, R. T., Coates, A. J., Wellbrock, A., et al. 2017, Carbon chain anions and the growth of complex organic molecules in Titan's ionosphere, *ApJL*, 844, L18

Hall, D. T., Feldman, P. D., McGrath, M. A., & Strobel, D. F. 1998, The Far-Ultraviolet Oxygen Airglow of Europa and Ganymede, *ApJL*, 499, 475

Hussmann, H., Sohl, F., & Spohn, T. 2006, Subsurface oceans and deep interiors of medium-sized outer planet satellites and large trans-neptunian objects, *Icarus*, 185, 258

Inoue, M., Ions ne gatifs forme s dans le cyanoge‘ne et lacide cyanhydrique, 1966, J. Chim. Phys., 63 1061-1071

Itikawa, Y. 2009, Cross sections for electron collisions with oxygen molecules, *Journal of Physical and Chemical Reference Data*, 38, 1

Johnson, R. E., & Sundqvist 1992, Electronic sputtering: from atomic physics to continuum mechanics, *Physics Today*, 28-36

Johnson, R. E., Killen, R. M., Waite, J. H., Jr., & Lewis, W. S., Europa's surface composition and sputter-produced ionosphere, 1998, *GRL*, 25, 3257

Khurana, K. K., Russell, C. T., & Dougherty, M. K. 2008, Magnetic portraits of Tethys and Rhea, *Icarus*, 193, 465

Khurana, K. K., Fatemi, S., Lindkvist, J., et al. 2017, The role of plasma slowdown in the generation of Rheas Alfven wings, *JGR*, 122, 1778

Lifshitz, Y., Kasi, S. R., Rabalais, J. W., & Eckstein, W. 1990, Subplantation model for film growth from hyperthermal species, *PRB*, 41, 10468

Martens, H. R., Reisenfeld, D. B., Williams, J. D., Johnson, R. E., & Smith, H. T. 2008, Observations of molecular oxygen ions in Saturn's inner magnetosphere, *GRL*, 35, L20103

Mary, et al. 2008, Absolute cross sections for dissociative electron attachment to acetylene and diacetylene, *Phys. Rev. A*, 77, 040701

McCord, T. B., Hansen, G. B., Clark, R. N., et al. 1998, Non-water-ice constituents in the surface material of the icy Galilean satellites from the Galileo near-infrared mapping spectrometer investigation, *JGR*, 103, 8603

Meeks, Z., Simon, S., & Kabanovic, S. 2016, A Comprehensive analysis of ion cyclotron waves in the equatorial magentsphere of Saturn, *PSS*, 129, 47

Mumma, M. J., & Charnley, S. B. 2011, The Chemical Composition of Comets - Emerging Taxonomies and Natal Heritage, *ARAA.*, 49, 471

Nordheim, T. A., Jones, G. H., Roussos, E., et al. Detection of a strongly negative surface potential at Saturn's moon Hyperion, 2014, *ARAA*, 41, 7011

Poppe, A. R., Samad, R., Halekas, J. S., et al. 2012, ARTEMIS observations of lunar pick-up ions in the terrestrial magnetotail lobes, *Geophys. Res. Lett.*, 39, L17104

Russell, C. T., Leisner, J. S., Arridge, C. S., Dougherty, M. K., & Blanco-Cano, X. 2006, Nature of magnetic fluctuations in Saturn's middle magnetosphere, *JGR*, 111, A12205

Roussos, E., Müller, J., Simon, S., et al. 2008, Plasma and fields in the wake of Rhea- 3-D hybrid simulation and comparison with Cassini data, *Ann. Geophys.*, 26, 619

Roussos, E., Krupp, N., Krüger, H., & Jones, G. H. 2010, Journal of Geophysical Research (Space Physics), 115, A08225

Roussos, E., Kollmann, P., Krupp, N., et al. 2012, Energetic electron observations of Rheas magnetospheric interaction, *Icarus*, 221, 116

Saito, Y., Yokota, S., Tanaka, T., et al. 2008, Solar wind proton reflection at the lunar surface: Low energy ion measurement by MAP-PACE onboard SELENE (KAGUYA), *GRL*, 35, L24205.

Santolík, O., Gurnett, D. A., Jones, G. H., et al. 2011, *Geophys. Res. Lett.,* , 38, L19204

Schenk, P., Hamilton, D. P., Johnson, R. E., et al. 2011, Plasma, plumes and rings: Saturn system dynamics as recorded in global color patterns on its midsize icy satellites, *Icarus*, 211, 740

Schippers, P., André, N., Johnson, R. E., et al. 2009, Identification of photoelectron energy peaks in Saturn's inner neutral torus, Journal of Geophysical Research (Space Physics), 114, A12212

Scipioni, F., Tosi, F., Stephan, K., et al. 2014, Spectroscopic classification of icy satellites of Saturn II: Identification of terrain units on Rhea, *Icarus*, 234, 1.

Simon, S., Kriegel, H., Saur, J., et al. 2012, Analysis of Cassini magnetic field observations over the poles of Rhea, Journal of Geophysical Research (Space Physics), 117, A07211

Sittler, E. C., Johnson, R. E., Jurac, S., et al. 2004, Pickup ions at Dione and Enceladus-Cassini Plasma Spectrometer simulations, *JGR*, 109, A01214.

Stephen, Pekol. 2000, Absolute calibration of a multichannel plate detector for low energy O, O, and O+, *Rev. Sc. Instr.*, 71, 1355.

Stephan, K., Jaumann, R., Wagner, R., et al. 2010, Dione's spectral and geological properties, *Icarus*, 206, 631

Stephan, K., Jaumann, R., Wagner, R., et al. 2012, he Saturnian satellite Rhea as seen by Cassini VIMS, *PSS*, 61, 142.

Tang, et al., O- ESD from O2 monolayers physisorbed on graphite: a surface mediated mechanism, 1996, *Zeitschrift fr Physik D Atoms, Molecules and Clusters*, 38, 41-44.

Taylor, et al. 2017, Modelling, analysis and interpretation of photoelectron energy spectra at Enceladus observed by Cassini, *JGR*, doi:10.1002/2017JA024536, in press.

Teolis, B. D., Jones, G. H., Miles, P. F., et al. 2010, Cassini finds an oxygen-carbon dioxide atmosphere at Saturns icy moon Rhea, *Science*, 330, 1813

Teolis, B. D., & Waite, J. H. 2016, Dione and Rhea seasonal exospheres revealed by Cassini CAPS and INMS, *Icarus*, 272, 277

Tokar, R. L., Johnson, R. E., Thomsen, M. F., et al. 2012, Detection of exospheric O2+ at Saturn's moon Dione, *GRL*, 39, L03105

Tortora, P., Zannoni, M., Hemingway, D., et al. 2016, Rhea gravity field and interior modeling from Cassini data analysis, *Icarus*, 264, 264

Wu, C. S., & Davidson, R. C. 1972, Electromagnetic instabilities produced by neutral-particle ionization in interplanetary space, *JGR*, 77, 5399

Wilson, R. J., Tokar, R. L., Kurth, W. S., & Persoon, A. M. 2010, Properties of the thermal ion plasma near Rhea as measured by the Cassini plasma spectrometer (IMS), *JGR*, 115, A05201

Wilson, R. J., Bagenal, F., & Persoon, A. M. 2017, Journal of Geophysical Research (Space Physics), 122, 7256

Young, D. T., et al. 2013, Cassini Plasma Spectrometer Investigation, Space Science Reviews, *SSR*, 114, 1-112

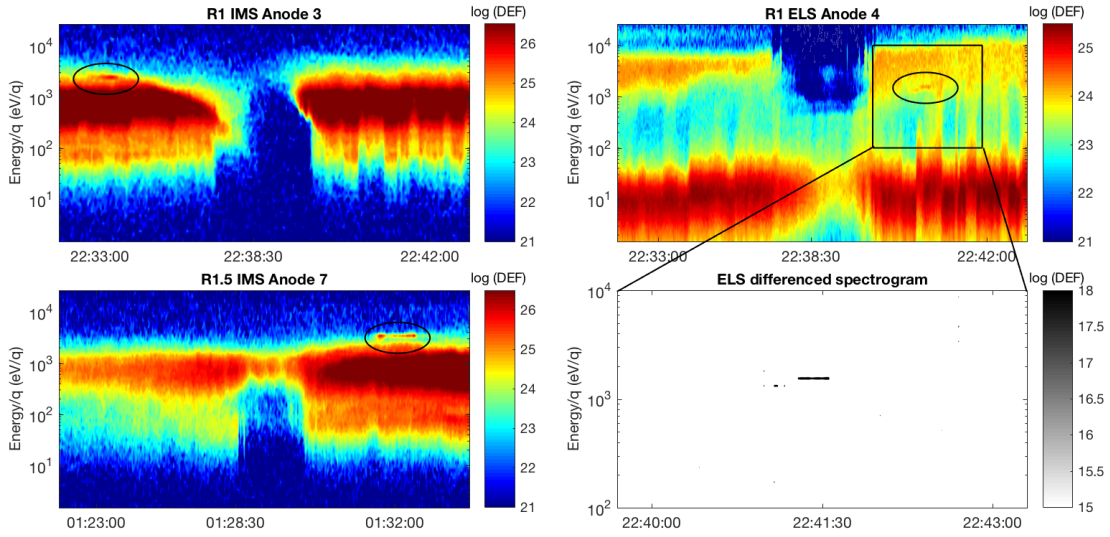

Figure 1. The left-hand panels show CAPS IMS differential energy flux (DEF) spectrograms acquired during the R1 and R1.5 encounters with Rhea and the right-hand panels CAPS ELS DEF spectrogram acquired during the R1 encounter. The IMS pickup ion detections are encircled at 22:33:00 during R1 at ∼2.5 keV and 01:33:00 during R1.5 at ∼3.5 keV. The negative pickup ion detections are evident at 22:41:30 at ∼1.5 keV. The lower right-hand panel shows a differenced plot of the ELS data which shows a negatively charged pickup ion signature similar in appearance to the positive pickup ion signatures.

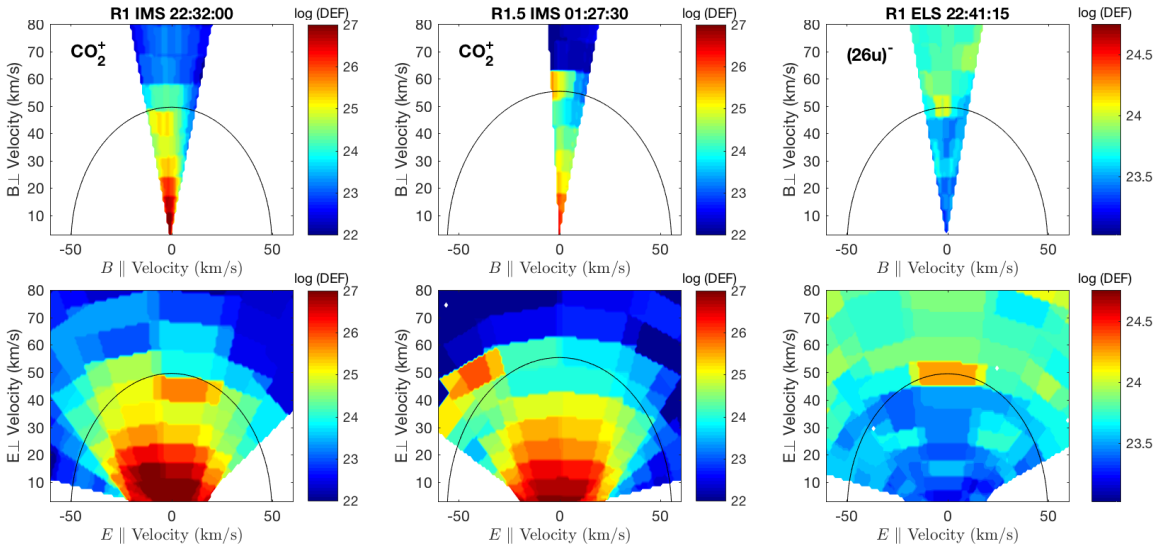

Figure 2. The CAPS data are converted into velocity space assuming CO_2^+ (left and centre panels) and mass 26 u (right-hand panels). These are projected into planes parallel and perpendicular to the magnetic field and $-v \times B$ electric field for a single energy sweep. A linear interpolation is used for overlapping FOVs which dilutes the detections when projected relative to the magnetic field. The geometrical look directions are used which, combined with each anodes 20° width, smears the detections in the parallel and anti-parallel directions. The pickup velocity ring-contour are overlaid.

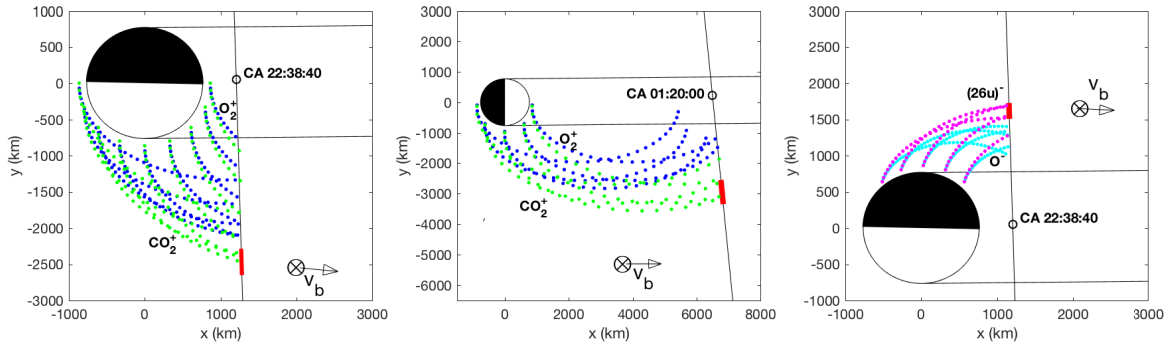

Figure 3. Nominal trajectories of outflowing O_2^+ (blue) and CO_2^+ (green) during R1 in the left-hand panel and during R1.5 in the centre panels. Outflowing O^- (cyan) and negative ions of 24u (magenta) are shown during R1 in the right-hand panel. The trajectories are calculated based upon Cassini plasma and field measurements at the time of detection and displayed in a Rhea centred coordinate system. The nominal corotational wake and approximate sunlit regions of Rhea are marked and times along Cassini's trajectory where the pickup ions were detected are marked red. The pickup ion trajectories originate within 100 km of Rhea's surface where increased neutral abundances are anticipated.

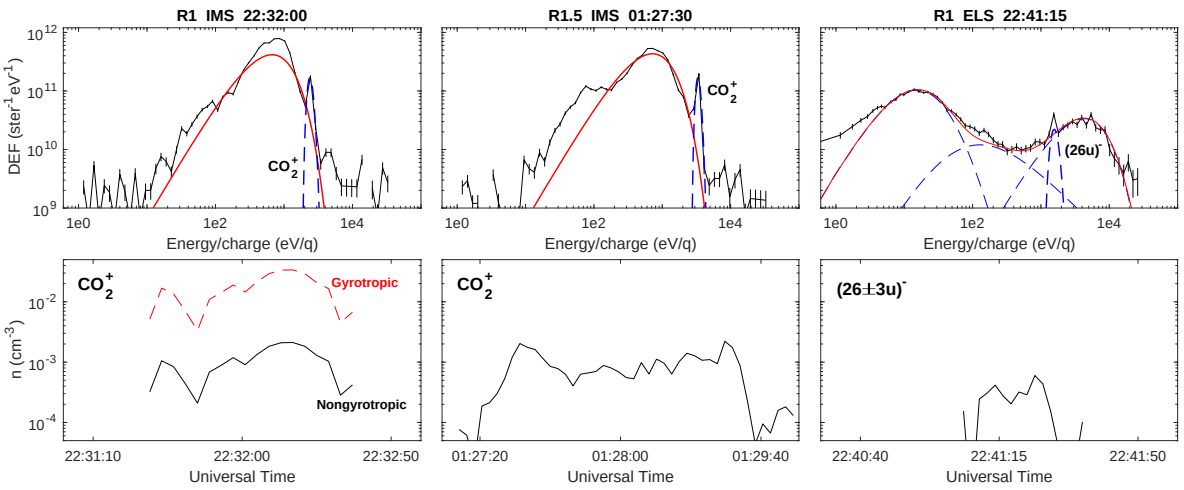

Figure 4. The top panels show an IMS and ELS spectrum from each of the pickup ion detections identified in Figure 1. The IMS background plasma is fitted to using Maxwellian velocity distributions for water-group ions and the ELS spectra is fitted using a low, medium and high energy kappa distributions. The lower panels show the calculated alongtrack densities.